Journal of Medicinal Chemistry

Brief Article

pubs.acs.org/jmc

One-Pot Synthesis of Vinca Alkaloids−Phomopsin Hybrids

Olga Gherbovet,[†] Claire Coderch,[‡] María Concepción García Alvarez,[†] Jérôme Bignon,[†] Sylviane Thoret,[†] Françoise Guéritte,[†] Federico Gago,[‡] and Fanny Roussi*[,†]

[†]Centre de Recherche de Gif, Institut de Chimie des Substances Naturelles, UPR 2301 du CNRS, Avenue de la Terrasse, 91198, Gif-sur-Yvette Cedex, France

[‡]Área de Farmacología, Departamento de Ciencias Biomédicas, Universidad de Alcalá, 28871 Alcalá de Henares, Madrid, Spain

Supporting Information

ABSTRACT: Hybrids of vinca alkaloids and phomopsin A have been elaborated with the aim of interfering with the "vinca site" and the "peptide site" of the vinca domain in tubulin. They were synthesized by an efficient one-pot procedure that directly links the octahydrophomopsin lateral chain to the velbenamine moiety of 7′-*homo*-anhydrovinblastine. In their modeled complexes with tubulin, these hybrids were found to superimpose nicely on the tubulin-bound structures of vinblastine and phomopsin A. This good matching can account for the fact that two of them are very potent inhibitors of microtubules assembly and are cytotoxic against four cancer cell lines.

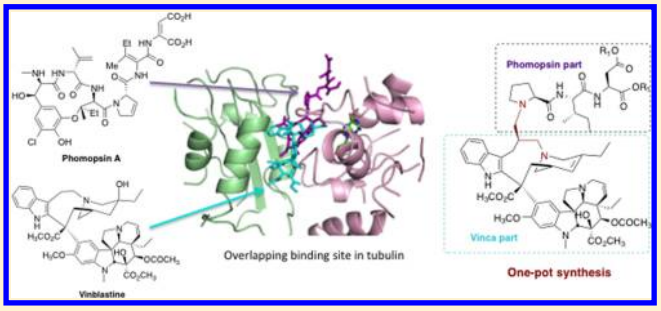

Cancer is characterized by uncontrolled cell proliferation and inappropriate cell survival. Microtubules play an important role in these cellular processes and have been one of the most efficacious targets for tumor chemotherapy. They are dynamic polymers made of heterodimers of α and β tubulin. Microtubule-binding molecules, a highly important class of anticancer agents, are generally derivatives of intricate natural products. They interfere with assembly or disassembly of microtubules by suppressing microtubule dynamics required for mitotic spindle function in rapidly dividing cells. In this way, they induce a cascade of events causing cells to commit suicide, that is, to undergo apoptosis or programmed cell death.[1]

Conventionally, microtubule-binding drugs are classified as stabilizing or destabilizing agents.[2] Among the assembly inhibitors, the vinca alkaloids (Figure 1) are highly potent antimitotic drugs that prevent tubulin polymerization into microtubules. Vinblastine **1** and vincristine **2**, isolated in the late 50s, and their synthetic derivatives vindesine **3**, vinorelbine **4**, and vinflunine **5** are used extensively in cancer chemotherapy.

Vinca alkaloids bind near the GTP-binding site in the "vinca site" of the so-called vinca domain. Atomic details about this "vinca site" were gained when Knossow et al. published the X-ray structure of vinblastine **1** bound to the tubulin-stathmin: RB3-SLD complex ((Tc)2R).[3] They showed that it is located at the interface between two tubulin heterodimers. Vinblastine is oriented so that velbenamine and vindoline moieties interact with the β1 monomer and the α2 monomer of the next heterodimer, velbenamine being close to the GTP/GDP nucleotide exchange site of the β1 subunit.

Other molecules are known to bind within the tubulin vinca domain. Since their binding site partly coincides with that of

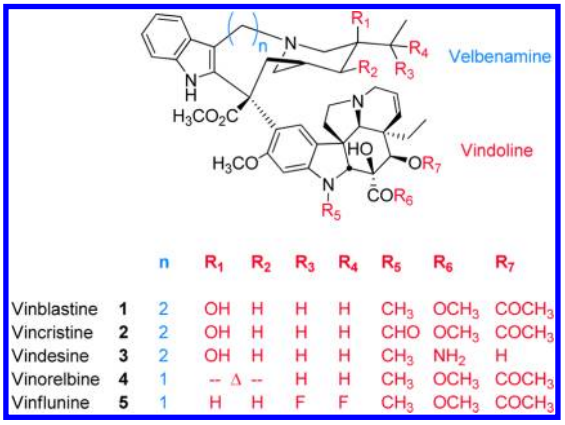

	n	R_1	R_2	R_3	R_4	R_5	R_6	R_7
Vinblastine **1**	2	OH	H	H	H	CH_3	OCH_3	$COCH_3$
Vincristine **2**	2	OH	H	H	H	CHO	OCH_3	$COCH_3$
Vindesine **3**	2	OH	H	H	H	CH_3	NH_2	H
Vinorelbine **4**	1	-- Δ --		H	H	CH_3	OCH_3	$COCH_3$
Vinflunine **5**	1	H	H	F	F	CH_3	OCH_3	$COCH_3$

Figure 1. Vinca alkaloids currently used in chemotherapy.

the vinca alkaloids, and most of them are peptides, they are considered to occupy the "'peptide site"' of the vinca domain.[2] This is the case for the antimitotic cyclopeptide phomopsin A **6**,[4] a hexapeptide that contains a 13-membered cyclic moiety and a lateral chain of three dehydroamino acids (Figure 2). **6** and unnatural *rac*-octahydrophomopsin A **7**[5] are very potent tubulin assembly inhibitors (IC_{50} of 0.56 and 0.40 μM, respectively) but are relatively weak cytotoxic agents.

Phomopsin A **6** was also cocrystallized with tubulin.[6] Superimposition of **1** and **6** binding sites revealed that they substantially overlap. The velbenamine moiety of **1** and the macrocyle of **6** fill the same areas that define the "vinca site",

Received: April 3, 2014

   dx.doi.org/10.1021/jm500530v | *J. Med. Chem.* XXXX, XXX, XXX−XXX

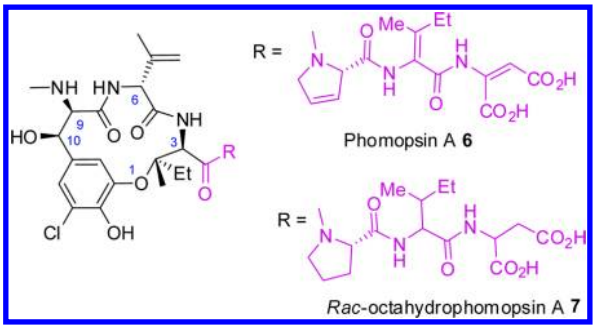

Figure 2. Phomopsin A **6** and *rac*-octahydrophomopsin A **7**.

whereas the vindoline moiety of **1** and the lateral chain of **6** accommodate in opposite directions. In particular, phomopsin A gives rise to multiple contacts with $Tyr_{\beta 224}$, one of the residues sandwiching the GDP/GTP nucleotide exchangeable site (Figure 3).

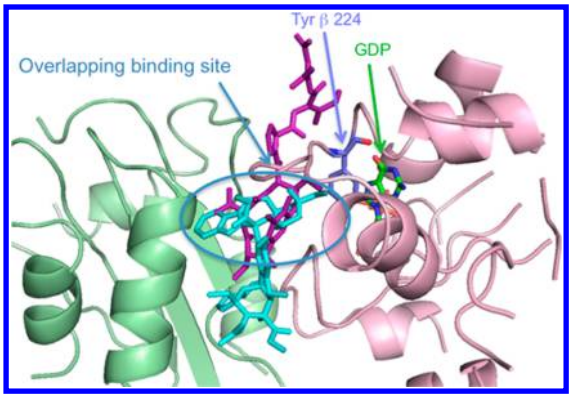

Figure 3. Superimposition of vinblastine (blue) and phomopsin A (purple) in their respective binding sites in tubulin which define the "vinca domain" (green, α_2-subunit; pink, β_1-subunit).

These noteworthy observations urged us to elaborate hybrids of **1** and **6** with the idea of obtaining molecules that could interfere with the "peptide" and the "vinca" sites simultaneously and addressing the question of whether the biological activities of the resulting compounds would be improved over those of the parent molecules.

So far, we have reported the synthesis of two series of vinca–phomopsin hybrids (Figure 4). Hybrids of the first generation **8** linked the phomopsin lateral chain to the tertiary amine of the velbenamine moiety of anhydrovinblastine and vinorelbine.[7] Although very active, molecular modeling showed that the absolute configuration of the quaternary nitrogen forces the phomopsin A lateral chain to orientate into a pocket different from that of the native compound. The second generation of vinca–phomopsin hybrids **9**, with a correct orientation of the phomopsin A lateral chain and a simplified velbenamine moiety, was found to be totally inactive.[8]

In this paper, we report the synthesis of a new family of 7′-*homo*-anhydrovinblastine and phomopsin hybrids **10** by means of a one-step procedure saving the four-ring structure of the velbenamine upper part and controlling the orientation of the inserted lateral chain. To achieve this goal, we used an original and highly selective insertion reaction of activated alkynes into the gramine bridge of vinorelbine **4**, which was recently worked out in our group.[9] This insertion reaction led to highly active diester or ester amide 7′-*homo*-anhydrovinblastine derivatives

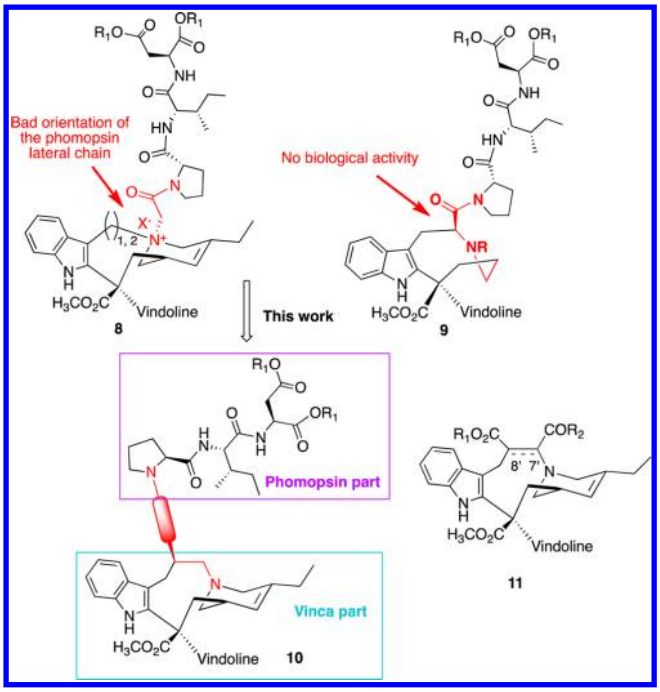

Figure 4. Envisaged hybrids of 7′-*homo*-vinblastine and phomopsin **10**.

11. So far, the 8′ position did not appear to tolerate bulky groups: with a methyl ester at 8′, compounds are highly active on tubulin but totally inactive if 8′ carries an ethyl or a benzyl ester.[9] Anyway, we postulated that using a more flexible linker in 8′ could favor accommodation of the phomopsin lateral chain in tubulin.

Our strategy relied on the elaboration of an aldehyde intermediate **12**, obtained in one step by an enlargement reaction of vinorelbine **4**, that could lead to the desired hybrids **13** by means of a reductive amination with peptide chains of various lengths (ProOMe, ProIleOMe, and ProIleAsp$(OBn)_2$) corresponding to those of phomopsin A lateral chain (Scheme 1).

Scheme 1. Envisaged Synthetic Pathway

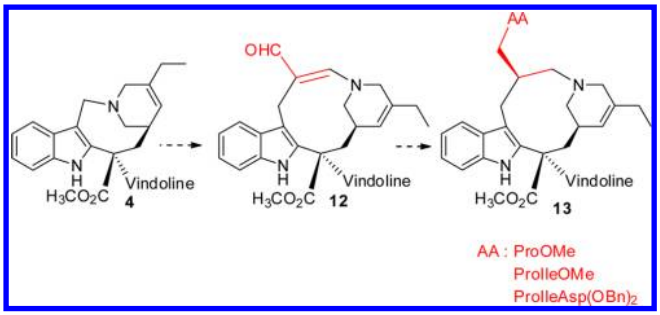

To obtain aldehyde **12**, commercial 3-(trimethylsilyl)-propynal was reacted with vinorelbine **4** in acetonitrile at room temperature for 2 h. The insertion reaction occurs probably by a Michael addition of the tertiary amine of **4** on the acetylene, generating a zwitterion **14**. It would lead to the reactive alkylideneindoleninium ion **15** after a spontaneous fragmentation of the gramine bridge. This ion could then be trapped intramolecularly to give inserted **16**. Nevertheless, this compound was not observed and the deprotected **12** was formed directly (20%). To increase the yield of this reaction,

dx.doi.org/10.1021/jm500530v | J. Med. Chem. XXXX, XXX, XXX–XXX

desilylation agents (TBAF, AgF) and various bases (DMA, K_2CO_3) were screened to favor the in situ deprotection. Finally, using 3 equiv of DMA at room temperature for 3 h increased the yield to 36% (Scheme 2).

Scheme 2. Synthesis of Aldehyde 12[a]

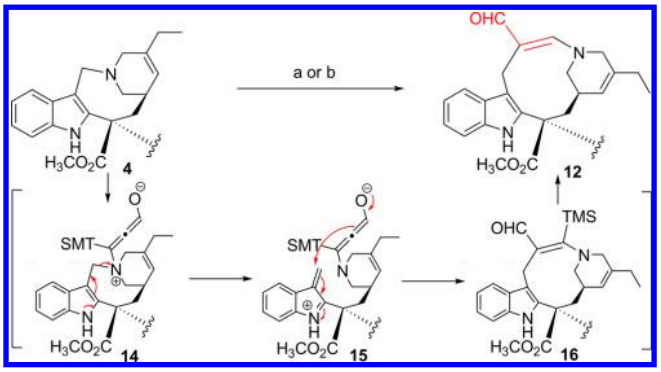

[a]Reagents and conditions: (a) 3-(trimethylsilyl)propynal, CH_3CH, 2h, rt, 20%; (b) 3-(trimethylsilyl)propynal, CH_3CN, 2 h, rt, then DMA, 3 h, rt, 36%.

Reductive aminations on **12** were then considered to obtain the desired hybrids (Table 1). As *rac*-octahydrophomopsin A **7** is as potent as phomopsin A **6** on tubulin and the synthesis of the phomopsin unsaturated tripeptide side chain requires a multistep procedure,[10] we made peptide chains containing natural L-proline, L-isoleucine, and L-aspartic acid. Commercially available Pro-OMe **17** was used, whereas Pro-Ile-OMe **18** and Pro-Ile-Asp-$(OBn)_2$ **19** were synthesized by classical peptide coupling.[7]

Table 1. Synthesis of Hybrids 20–22[a]

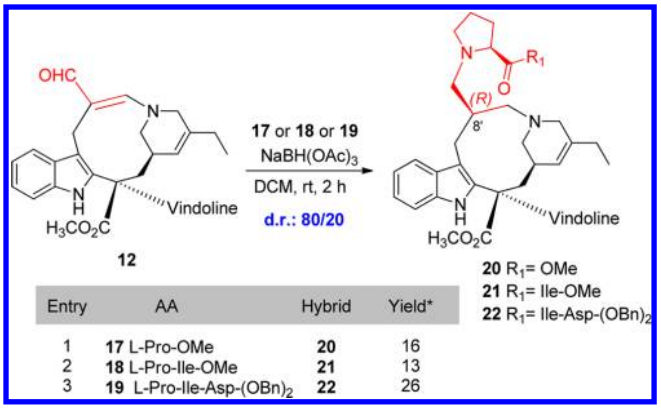

Entry	AA	Hybrid	Yield*
1	**17** L-Pro-OMe	**20**	16
2	**18** L-Pro-Ile-OMe	**21**	13
3	**19** L-Pro-Ile-Asp-$(OBn)_2$	**22**	26

[a]The asterisk (*) indicates isolated yield of the major diastereomer.

Three hybrids were obtained with a ratio of 80:20. Note that calculated yields correspond solely to the major diastereoisomer, as it was the only one that could be isolated by column chromatography. As loss of material was observed during the purification, yields were estimated satisfying with regard to the molecular complexity of the synthesized compounds.

If 1.8 equiv of peptide could be used, an excess of sodium triacetoxyborohydride (2.6 equiv) was employed, as a double reduction of two iminium species **23** and **24** occurs during the reaction (Scheme 3).

Scheme 3. Double Reduction of Iminium Species 23 and 24 to Compounds 20–22

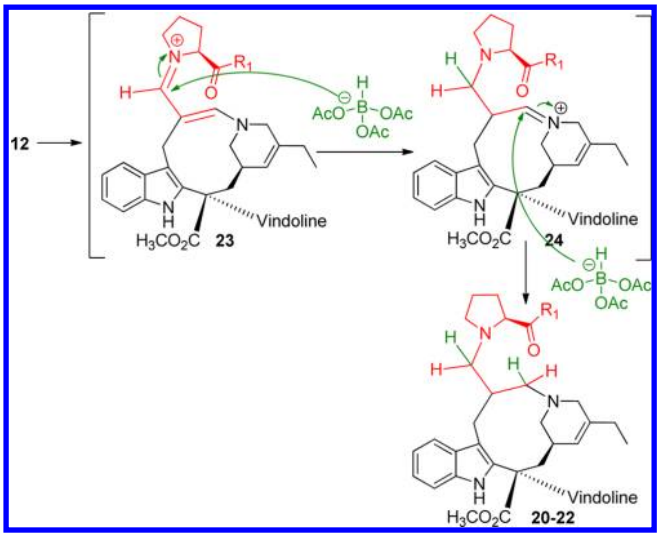

To avoid the purification of aldehyde **12**, which is not very stable on silica gel, a one-pot synthesis of hybrids **20–22** was considered. Thus, **4** was reacted with 1.1 equiv of 3-(trimethylsilyl)propynal at room temperature. After 2 h of stirring necessary for the formation of aldehyde **12**, an amount of 1.75 equiv of peptide **17** or **18** or **19** was added, followed by 2.6 equiv of sodium triacetoxyborohydride in solution in dichloromethane (Table 2). The diastereoisomeric *ratio* remained the same and once again; only the major diastereoisomer could be isolated. It is important to note that five different reactions (insertion, silyl group deprotection, amination, and double reduction of iminiums **23** and **24**) take place in the same flask.

Table 2. One-Pot Synthesis of Hybrids 20–22[a]

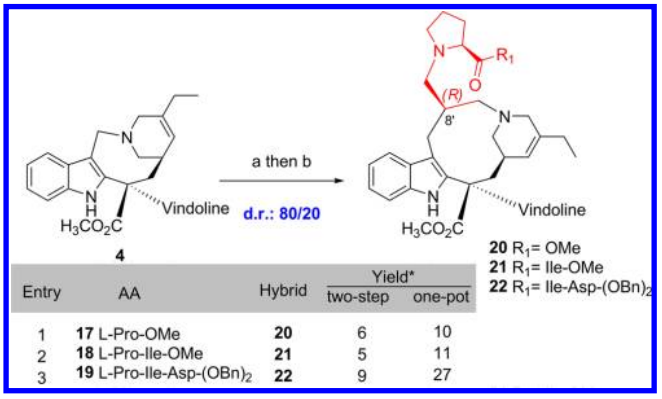

Entry	AA	Hybrid	Yield* two-step	Yield* one-pot
1	**17** L-Pro-OMe	**20**	6	10
2	**18** L-Pro-Ile-OMe	**21**	5	11
3	**19** L-Pro-Ile-Asp-$(OBn)_2$	**22**	9	27

[a]Reagents and conditions: (a) 3-(trimethylsilyl)propynal, CH_3CN, 2 h, rt; (b) AA, $NaBH(OAc)_3$, DCM, rt, 2 h. The asterisk (*) indicates isolated yield of the major diastereomer.

The configuration of the new steric center for **20–22** was determined by NOE experiments. For example, for **22**, correlations could be observed between H-12′ and H-9′α, H-12′ and H-8′, H-1′α and H-2′ on the lower face and between H-1′β and H-9′β on the upper face. In parallel, molecular dynamics simulations were run for the two possible (8-*R*) and (8-*S*) epimers of **22**. They confirmed that such correlations are only consistent with a (8-*R*) configuration (Figure 5). This *R* configuration at C-8′ for the isolated hybrids **20–22**

dx.doi.org/10.1021/jm500530v | J. Med. Chem. XXXX, XXX, XXX–XXX

corresponds to those essential for a correct orientation of the lateral chain in the binding site of tubulin.

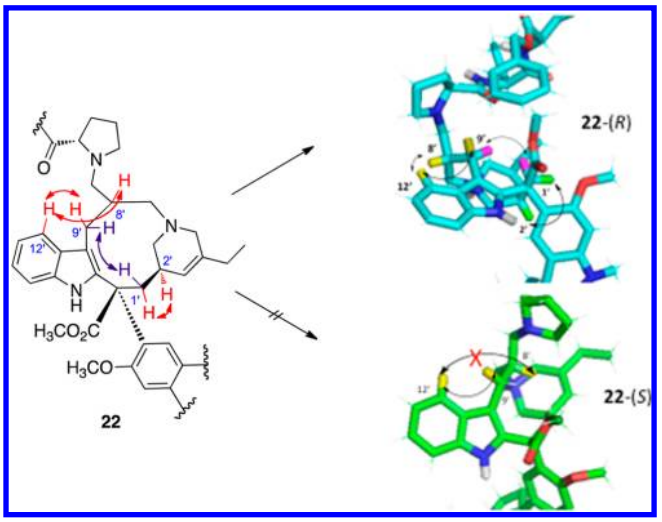

Figure 5. NOE correlations for **22**.

Compounds **20**–**22** were evaluated for inhibition of tubulin polymerization (Table 3). Compounds **20** and **21** displayed

Table 3. Biological Activities of Hybrids 20–22

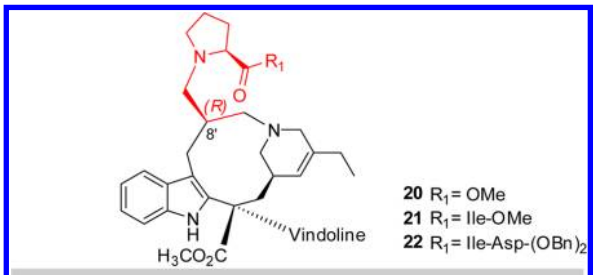

	1 (VLB)	4 (VNL)	20	21	22
$IC_{50\text{-tubuline}}$ (μM)[a]	2.1	0.6	1.0	2.7	>100
$IC_{50\text{-HCT116}}$ (nM)[b]	3.5	35	700	1000	nd
$IC_{50\text{-U87}}$ (nM)[b]	1.0	2	25	400	nd
$IC_{50\text{-K562}}$ (nM)[b]	2.7	3.5	120	250	nd
$IC_{50\text{-MCF7}}$ (nM)[b]	0.7	4	230	800	nd

[a] $IC_{50\text{-tubulin}}$ is the concentration of a compound that inhibits 50% of the rate of microtubule assembly (concentration in tubulin, 3 mg/mL). [b] $IC_{50\text{-cell line}}$ measures the drug concentration required for the inhibition of 50% cell proliferation after 72 h of incubation.

significant inhibitory activity on microtubule assembly. Compound **20** was even more potent than **1** and slightly less potent than **4**, and **21** was almost as active as **1**. It clearly indicates that the phomopsin side chain has a synergistic effect on activity because we have shown previously that insertion of inappropriate bulky groups at 8′ lead to inactive compounds.[9]

Nevertheless, the size of the added groups should not be too large in view of the total loss of activity observed for **22**. These results confirm that the 8′ position can tolerate bulky groups when a methylene linker is used and go along the same line as the molecular modeling results.

Even if it is less cytotoxic than vinorelbine **4** and vinblastine **1**, **20** was found very active against the four tested cell lines mainly on U87 glioblastoma, K562 erythromyeloblastoid leukemia, and MCF-7 breast cancer cells.

Molecular modeling was undertaken on **20** and **21** to determine whether they occupy the entire vinca domain in comparison with vinblastine and phomopsin A. The structures of **20** and **21** were assembled in a potential binding conformation at the $\beta_2\alpha_1$-tubulin interface, and molecular dynamics (MD) simulations were carried out. All ligands were located between the GDP-bound β-tubulin subunit of the "bottom" heterodimer (β_1) and the GTP-Mg^{2+}-bound α-tubulin subunit of the "top" heterodimer (α_2).[3] Complex relaxation and enhanced sampling over the course of the MD trajectories resulted in improved adaptation of each ligand within the binding site and provided details of the intermolecular interactions.

As postulated, the *R* configuration at C-8′ for the hybrids **20**–**22** enables a correct orientation of the lateral chain in the binding site of tubulin. Consequently, as for that of phomopsin A, both are oriented in the direction of $Tyr_\beta224$ and GDP. In addition, for **21**, the carbonyl amide of proline establishes a hydrogen bonding interaction with the OH of $Tyr_\beta224$ (Figure 6b, red circle) that pushes isoleucine out of the $\beta_2\alpha_1$-tubulin interdimer.

The superimposition of **20**, **1**, and **6** in their respective binding sites clearly indicates that the hybrid occupies the whole vinca domain, as its lateral chain superimposes perfectly to that of **6**. The only difference resides in the conformation of the amino acids chain that is much flatter in the case of phomopsin A, because of the presence of dehydroamino acids (Figure 7).

In conclusion, three new 7′-*homo*-anhydrovinblastine and phomopsin hybrids carrying peptide chains of different lengths at position 8′ were synthesized starting from vinorelbine **4** using a selective and efficient one-pot procedure. Compound **20** was shown to inhibit microtubule assembly with an IC_{50} similar to those of **1** and **4** and to display good cytotoxicity against four cancer cell lines. Molecular modeling studies indicated that the lateral chain of **20** is lodged within the same pocket that is occupied by natural phomopsin A **6**, but the latter is less flexible because of the presence of unsaturated amino acids. These results pave the way to the elaboration of more potent vinca–peptide hybrids by varying the nature and the bulk of the peptide chain. This is why, thereafter, the synthesis of hybrids with a more rigid lateral chain is envisaged to determine the contribution of the rigidity of the peptidic chain to the biological activity. Likewise, it seems worthwhile, according to molecular modeling studies, to use hydrophilic amino acids at the end of the lateral chain to improve the tubulin binding affinity. Additionally, it is known that a simplification of the vindoline part of the vinca alkaloids leads to inactive compounds.[7b,11] The elaboration of simplified vinblastine–phomospin hybrids using this insertion reaction could be considered as a proof of concept: if the added peptide chains have a real influence on activity, a new family of antimitotic compounds could be elaborated. Contrariwise, if they have no impact, a simplification of the vinblastine moiety should induce loss of activity.

EXPERIMENTAL SECTION

General Information. Vinorelbine tartrate was a gift from the Institut de Recherche Pierre Fabre. All reactions were performed in oven-dried glassware under an argon atmosphere. ^1H NMR and ^{13}C NMR spectra were recorded on a Bruker ARX500 or Avance 600 spectrometer. Tested **20**–**22** possess a purity of ≥95% that was

dx.doi.org/10.1021/jm500530v | J. Med. Chem. XXXX, XXX, XXX–XXX

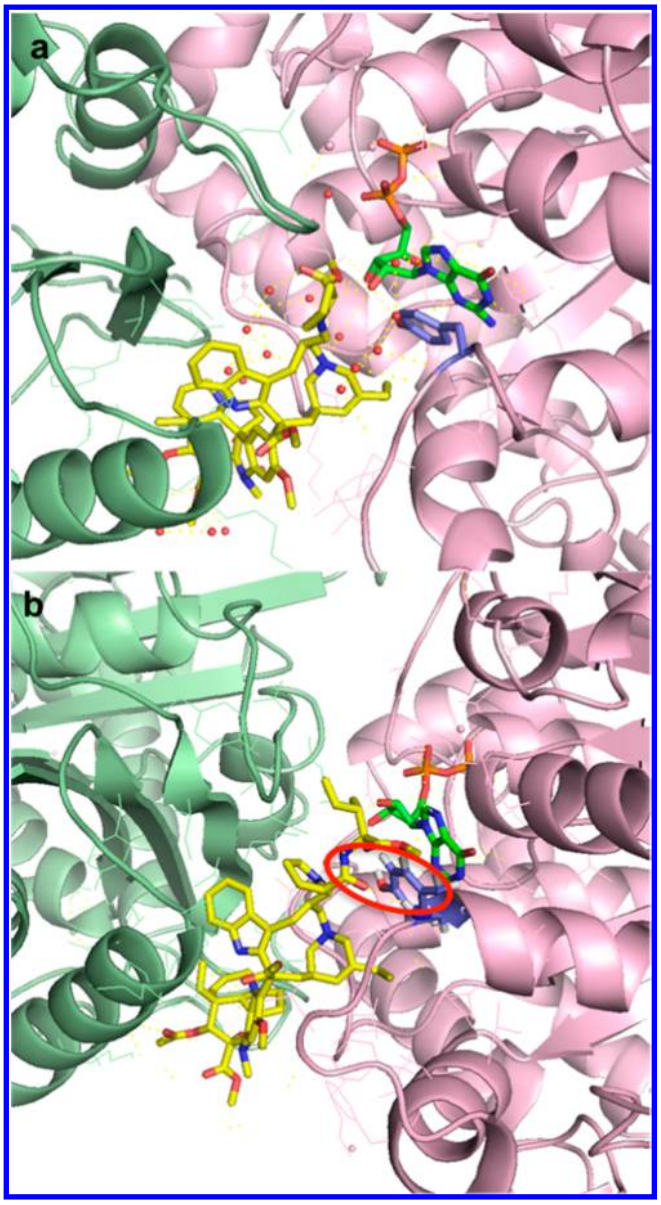

Figure 6. PyMOL cartoons and sticks representation of (a) hybrid **20** (yellow) and (b) hybrid **21** (yellow), Tyr β224 (blue), and GDP (green and orange) bound at the $\beta_1\alpha_2$ tubulin interdimer interface.

determined by UPLC using a C18 column (2.1 mm × 50 mm) and a gradient of water/acetonitrile from 95:5 to 0:100.

Compound 12. 3-(Trimethylsilyl)propynal (10 μL, 0.07 mmol, 1.1 equiv) and dimethylamine 2 M (56 μL) were added to a solution of vinorelbine (50 mg, 0.065 mmol, 1 equiv) in 0.5 mL of anhydrous acetonitrile. After the mixture was stirred for 2 h at room temperature, the solvent was evaporated under reduced pressure. The resulting residue was purified by column chromatography on silica gel using ethyl acetate/acetone (1:0 to 4:1) to afford **12** (20 mg, 36% yield). ^{1}H NMR (500 MHz, CD_3CN): δ (ppm) 8.99 (s, 1H, H-25′), 8.22 (s, 1H, H-17′), 7.89 (s, 1H, OH), 7.54 (d, J = 7.8 Hz, 1H, H-12′), 7.16 (d, J = 7.8 Hz, 1H, H-15′), 7.03 (s, 1H, H-14), 7.00 (s, 1H, H-7′), 6.97 (t, J = 7.8 Hz, 1H, H-14′), 6.89 (t, J = 7.8 Hz, 1H, H-13′), 6.31 (s, 1H, H-17), 5.79 (dd, J = 10.4 and 3.9 Hz, 1H, H-7), 5.44 (d, J = 2.6 Hz, 1H, H-3′), 5.29 (s, 1H, H-4), 5.23 (d, J = 10.4 Hz, 1H, H-6), 4.2 (d, J = 15.8 Hz, 1H, H-9′β), 3.72 (d, J = 15.8 Hz, 1H, H-5′α), 3.68 (s, 3H, H-25), 3.64 (s, 1H, H-2), 3.64 (s, 3H, H-22), 3.59 (d, J = 15.8 Hz, 1H, H-9′α), 3.51 (s, 3H, H-24′), 3.48 (m, 1H, H-20′β), 3.47(d, J = 15.8 Hz, 1H, H-5′β), 3.36 (dd, J = 15.8 and 4.9 Hz, 1H, H-8β), 3.30 (m, 1H, H-10β), 3.09 (dd, J = 14.8 and 11,9 Hz, 1H, H-1′α), 2.72 (s, 1H, H-19), 2.70 (m, 1H, H-8α), 2.69 (s, 3H, H-23), 2.56 (dd, J = 14.5 and 4.3 Hz, 1H, H-20′α), 2.48 (m, 1H, H-10α), 2.22−2.15 (m, 2H, H-11α and H-11β), 2.18 (m, 1H, H-1′β), 2.08 (m, 1H, H-2′), 2.01 (s, 3H, H-27), 1.93 (m, 2H, H-21′), 1.73 (dd, J = 14.0 and 7.3 Hz, 1H, H-20α), 1.28 (dd, J = 14.0 and 7.3 Hz, 1H, H-20β), 0.95 (t, J = 7.3 Hz, 3H, H-22′), 0.54 (t, J = 7.3 Hz, 3H, H-21). ^{13}C NMR (125 MHz, CD_3CN): δ (ppm) 192.0 (C-25′), 174.7 (C-23′), 173.1 (C-24), 171.5 (C-26), 162.0 (C-7′), 159.8 (C-16), 154.5 (C-18), 139.8 (C-4′), 136.0 (C-16′), 132.7 (C-18′), 131.2 (C-6), 129.9 (C-11′), 125.5 (C-7), 125.4 (C-13), 124.7 (C-14), 124.4 (C-3′), 122.6 (C-14′), 120.5 (C-12′), 120.5 (C-15), 120.0 (C-13′), 115.3 (C-10′), 114.0 (C-8′), 111.9 (C-15′), 95.5 (C-17), 84.5 (C-2), 80.6 (C-3), 77.5 (C-4), 67.5 (C-19), 56.6 (C-22), 55.5 (C-19′), 55.1 (C-5′), 54.2 (C-12), 52.9 (C-24′), 52.7 (C-25), 51.8 (C-10), 51.6 (C-8), 50.7 (C-20′), 45.3 (C-11), 43.8 (C-5), 38.9 (C-23), 35.9 (C-1′), 34.7 (C-2′), 32.0 (C-20), 28.1 (C-21′), 21.3 (C-27), 20.7 (C-9′), 12.6 (C-22′), 8.7 (C-21). HRMS (ESI): calcd for $C_{48}H_{55}N_4O_9$ 831.3969, found 831.3990. $[\alpha]_D$ −60 ($CHCl_3$, c 1.0).

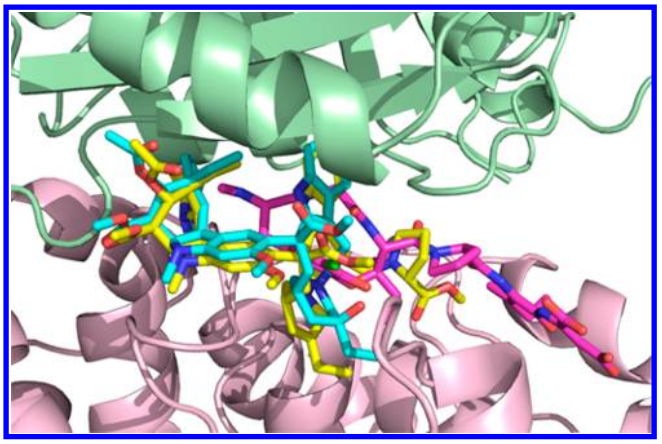

Figure 7. PyMOL cartoons and stick superimposition of **20** (yellow sticks), vinblastine **1** (blue sticks), and phomopsin A **6** (magenta sticks) in their "active conformation" within their respective binding sites.

General Procedure for the Synthesis of Hybrids 20−22. *Method 1.* To a solution of amine (0.04 mmol, 1.75 equiv) and aldehyde **12** (20 mg, 0.02 mmol, 1 equiv) in 0.2 mL of dichloromethane was added $NaBH(OAc)_3$ (13 mg, 0.06 mmol, 2.6 equiv) at room temperature. The mixture was stirred for 3 h at 0 °C. The resulting mixture was diluted with dichloromethane and washed with a saturated sodium carbonate solution. The organic layers were combined, washed with brine, dried over magnesium sulfate, and filtered. The solvents were removed under reduced pressure to provide the crude compound. Purification was carried out on silica gel using ethyl acetate/acetone (1:0 to 4:1) to afford desired compound **20** (3 mg, 16% yield) as a white solid.

Method 2. 3-(Trimethylsilyl)propynal (20 μL, 0.14 mmol, 1.1 equiv) was added to a solution of vinorelbine (100 mg, 0.13 mmol, 1 equiv) in 1 mL of anhydrous acetonitrile. After the mixture was stirred for 2 h at room temperature, amine (0.23 mmol, 1.75 equiv) and $NaBH(OAc)_3$ (70 mg, 0.33 mmol, 2.6 equiv) in 1 mL of dichloromethane were added at room temperature. The mixture was stirred for 3 h at room temperature. The resulting mixture was diluted with dichloromethane and washed with a saturated sodium carbonate solution. The organic layers were combined, washed with brine, dried over magnesium sulfate, and filtered. The solvents were removed under reduced pressure to provide the crude compound. Purification was carried out by column chromatography on silica gel using ethyl acetate/acetone (1:0 to 4:1), affording **20** (12 mg, 10% yield).

Compound 20. White solid, 16% yield (3 mg) by method 1, 10% yield (12 mg) by method 2. ^{1}H NMR (500 MHz, $CDCl_3$) δ (ppm) 7.93 (s, 1H, H-17′), 7.70 (d, J = 7.3 Hz, 1H, H-12′), 7.11−7.05 (m, 2H, H-14′ and H-15′), 7.04 (t, J = 7.3 Hz, 1H, H-13′), 6.84 (s, 1H, H-14), 6.11 (s, 1H, H-17), 5.83 (dd, J = 10.4 and 4.4 Hz, 1H, H-7), 5.50

dx.doi.org/10.1021/jm500530v | J. Med. Chem. XXXX, XXX, XXX−XXX

(s, 1H, H-4), 5.28 (d, J = 10.4 Hz, 1H, H-6), 5.16 (d, J = 4.2 Hz, 1H, H-3′), 3.78 (s, 3H, H-22), 3.77 (s, 3H, H-25), 3.72 (s, 1H, H-2), 3.70 (d, J = 10.2 Hz, 1H, H-9′β), 3.67 (s, 3H, H-32′), 3.55−3.49 (m, 1H, H-1′β), 3.51 (s, 3H, H-24′), 3.43−3.36 (m, 2H, H-8β and H-30′), 3.32−3.26 (m, 2H, H-5′β and H-10α), 3.16−3.13 (m, 1H, H-27′α), 3.04−2.98 (m, 1H, H-20′β), 2.96 (d, J = 13.6 Hz, 1H, H-5′α), 2.84−2.80 (m, 2H, H-8α and H-25′β), 2.74−2.71 (m, 1H, H-9′α), 2.70 (s, 1H, H-19), 2.68 (s, 3H, H-23), 2.69−2.64 (m, 1H, H-25′α), 2.63 (d, J = 9.9 Hz, H-7′β), 2.59 (d, J = 10.0 Hz, H-27′β), 2.44−2.38 (m, 2H, H-7′α and H-10β), 2.36−2.32 (m, 1H, H-8′), 2.22−2.17 (m, 2H, H-11), 2.14 (d, J = 14.0 Hz, 1H, H-1′α), 2.09 (s, 3H, H-27), 2.12−2.07 (m, 1H, H-29′α), 2.02−1.94 (m, 3H, H-20′α, H-28′β and H-29′β), 1.91−1.73 (m, 4H, H-20β, H-21′ and H-28′α), 1.41−1.31 (m, 1H, H-20α), 1.25−1.22 (m, 1H, H-2′), 0.94 (t, J = 7.0 Hz, 3H, H-22′), 0.83 (t, J = 7.0 Hz, 3H, H-21). ^{13}C NMR (125 MHz, $CDCl_3$) δ (ppm) 175.4 (C-31′), 174.5 (C-23′), 171.9 (C-24), 171.1 (C-26), 158.5 (C-16), 153.2 (C-18), 140.2 (C-4′), 135.3 (C-16′), 130.6 (C-18′), 130.3 (C-6), 130.3 (C-11′), 125.2 (C-14), 124.7 (C-7), 123.6 (C-3′), 123.5 (C-13), 122.0 (C-14′), 121.4 (C-15), 120.1 (C-12′), 118.8 (C-13′), 117.3 (C-10′), 110.6 (C-15′), 94.7 (C-17), 83.9 (C-2), 79.8 (C-3), 76.7 (C-4), 66.7 (C-30′), 66.4 (C-19), 61.0 (C-25′), 58.2 (C-5′), 56.5 (C-19′), 56.2 (C-22), 55.8 (C-7′), 54.3 (C-27′), 53.6 (C-12), 53.5 (C-20′), 52.5 (C-25), 52.4 (C-24′), 52.3 (C-32′), 51.1 (C-10), 50.7 (C-8), 45.0 (C-11), 43.1 (C-5), 41.1 (C-8′), 38.6 (C-23), 35.6 (C-2′), 34.6 (C-1′), 31.2 (C-20), 29.8 (C-29′), 27.8 (C-21′), 26.4 (C-9′), 24.0 (C-28′), 21.4 (C-27), 12.6 (C-22′), 8.8 (C-21). HRMS (ESI) calcd for $C_{54}H_{70}N_5O_{10}$ 948.5117, found 948.5223. $[\alpha]_D$ +6 ($CHCl_3$, c 0.1).

Compound 21. White solid, 13% yield (3 mg) by method 1, 11% yield (3 mg) by method 2. ^{1}H NMR (500 MHz, CD_3CN) δ (ppm) 8.30 (s, 1H, H-17′), 7.78 (d, J = 8.6 Hz, 1H, H-32′), 7.59 (d, J = 6.8 Hz, 1H, H-12′), 7.18 (d, J = 7.6 Hz, 1H, H-15′), 7.10 (s, 1H, H-14), 7.04 (t, J = 7.6 Hz, 1H, H-14′), 6.97 (t, J = 7.6 Hz, 1H, H-13′), 6.29 (s, 1H, H-17), 5.83 (dd, J = 9.9 and 4.7 Hz, 1H, H-7), 5.32 (d, J = 9.9 Hz, 1H, H-6), 5.25 (s, 1H, H-4), 5.19 (d, J = 5.6 Hz, 1H, H-3′), 4.30 (dd, J = 8.6 and 5.0 Hz, 1H, H-33′), 3.75 (s, 3H, H-39′), 3.69 (s, 3H, H-22), 3.68−3.64 (m, 1H, H-9′β), 3.58 (s, 3H, H-25), 3.56 (s, 1H, H-2), 3.49 (dd, J = 14.2 and 12.1 Hz, 1H, H-1′β), 3.44 (s, 3H, H-24′), 3.45−3.40 (m, 1H, H-7′α), 3.32 (dd, J = 15.8 and 5.3 Hz, 1H, H-8β), 3.20 (td, J = 9.3 and 4.7 Hz, 1H, H-10β), 3.10 (dd, J = 10.0 and 2.9 Hz, 1H, H-30′), 3.04 (d, J = 15.8 Hz, 1H, H-5′β), 2.98 (d, J = 12.2 Hz, 1H, H-20′β), 2.94−2.89 (m, 2H, H-5′α and H-25′β), 2.88 (s, 1H, H-19), 2.89−2.85 (m, 1H, H-9′α), 2.76 (d, J = 15.9 Hz, 1H, H-8α), 2.67 (s, 3H, H-23), 2.58 (dd, J = 12.5 and 5.5 Hz, 1H, H-25′α), 2.51−2.45 (m, 4H, H-7′β, H-27′, H-10α), 2.43−2.38 (m, 1H, H-8′), 2.19−2.15 (m, 1H, H-29′α), 2.09 (d, J = 14.2 Hz, 1H, H-1′α), 2.08−2.02 (m, 1H, H-11β), 1.98 (s, 3H, H-27), 1.96−1.92 (m, 1H, H-20′α), 1.93−1.88 (m, 3H, H-21′ and H-34′), 1.88−1.83 (m, 2H, H-11α and H-28′α), 1.83−1.78 (m, 2H, H-28′β and H-29′β), 1.68−1.63 (m, 1H, H-20α), 1.43−1.39 (m, 1H, H-35′α), 1.40−1.35 (m, 1H, H-20β), 1.21−1.17 (m, 1H, H-2′), 1.13−1.09 (m, 1H, H-35′β), 0.94 (t, J = 7.4 Hz, 3H, H-22′), 0.86 (d, J = 6.3 Hz, 3H, H-37′), 0.81−0.78 (m, 6H, H-36′ and H-21). ^{13}C NMR (125 MHz, CD_3CN) δ (ppm) 175.9 (C-38′), 175.5 (C-31′), 174.8 (C-23′), 173.0 (C-24), 171.8 (C-26), 159.4 (C-16), 154.8 (C-18), 141.4 (C-4′), 136.6 (C-16′), 133.2 (C-18′), 131.5 (C-6), 131.1 (C-11′), 125.7 (C-14), 125.7 (C-7), 124.8 (C-13), 124.4 (C-3′), 122.7 (C-14′), 122.3 (C-15), 120.5 (C-12′), 119.6 (C-13′), 116.6 (C-10′), 112.1 (C-15′), 95.1 (C-17), 84.4 (C-2), 80.8 (C-3), 77.5 (C-4), 69.5 (C-30′), 66.0 (C-19), 64.2 (C-25′), 58.8 (C-5′), 57.5 (C-27′), 57.4 (C-19′), 57.0 (C-33′), 56.4 (C-22), 55.8 (C-7′), 55.3 (C-20′), 54.5 (C-12), 52.9 (C-25), 52.8 (C-24′), 52.7 (C-39′), 51.3 (C-8), 50.7 (C-10), 45.9 (C-11), 44.0 (C-5), 42.5 (C-8′), 39.1 (C-23), 38.2 (C-34′), 36.9 (C-2′), 35.7 (C-1′), 32.0 (C-20), 31.5 (C-29′), 28.3 (C-21′), 27.0 (C-9′), 26.0 (C-35′), 25.5 (C-28′), 21.5 (C-27), 16.4 (C-37′), 12.9 (C-22′), 12.1 (C-36′), 9.0 (C-21). HRMS (ESI) calcd for $C_{60}H_{81}N_6O_{11}$ 1061.5958, found 1061.6012. $[\alpha]_D$ +4 ($CHCl_3$, c 0.1).

Compound 22. White solid, 26% yield (8 mg) by method 1, 27% yield (24 mg) by method 2. ^{1}H NMR (600 MHz, CD_3CN) δ (ppm) 8.30 (s, 1H, H-17′), 7.78 (d, J = 8.6 Hz, 1H, H-32′), 7.59 (d, J = 6.8 Hz, 1H, H-12′), 7.30−7.23 (m, 10H, H-45′−H-49′ and H-53′−H-57′), 7.13 (d, J = 8.6 Hz, 2H, H-15′ and H-39′), 7.02 (s, 1H, H-14), 6.97 (t, J = 8.6 Hz, 1H, H-14′), 6.91 (t, J = 8.6 Hz, 1H, H-13′), 6.25 (s, 1H, H-17), 5.76 (dd, J = 10.3 and 4.6 Hz, 1H, H-7), 5.26 (d, J = 10.3 Hz, 1H, H-6), 5.23 (s, 1H, H-4), 5.09 (d, J = 4.7 Hz, 1H, H-3′), 5.00 (s, 2H, H-43′), 4.94 (d, J = 4.3 Hz, 2H, H-51′), 4.81 (q, J = 6.7 Hz, 1H, H-40′), 4.12 (dd, J = 8.3 and 6.1 Hz, 1H, H-33′), 3.69 (s, 3H, H-22), 3.66 (s, 3H, H-25), 3.64 (d, J = 13.3 Hz, 1H, H-9′β), 3.52 (s, 1H, H-2), 3.43 (d, J = 10.3 Hz, 1H, H-1′β), 3.41 (s, 3H, H-24′), 3.30 (t, J = 6.8 Hz, 1H, H-7′α), 3.23 (dd, J = 16.4 and 4.9 Hz, 1H, H-8β), 3.13 (td, J = 9.3 and 4.4 Hz, 1H, H-10β), 3.08 (dd, J = 9.5 and 3.2 Hz, 1H, H-30′), 2.98 (d, J = 15.1 Hz, 1H, H-5′α), 2.91 (d, J = 11.6 Hz, 1H, H-20′β), 2.89−2.84 (m, 1H, H-5′β), 2.83 (d, J = 12.0 Hz, 1H, H-25′β), 2.80 (dd, J = 17.7 and 5.5 Hz, 1H, H-41′β), 2.78 (s, 1H, H-19), 2.76−2.74 (m, 1H, H-9′α), 2.72 (dd, J = 17.7 and 5.5 Hz, 1H, H-41′α), 2.66−2.64 (m, 1H, H-8α), 2.63 (s, 3H, H-23), 2.56 (dd, J = 12.0 and 6.7 Hz, 1H, H-25′α), 2.50−2.44 (m, 2H, H-7′β and H-27′β), 2.42−2.36 (m, 2H, H-10α and H-27′α), 2.31−2.26 (m, 1H, H-8′), 2.13−2.09 (m, 1H, H-29′β), 2.07 (d, J = 10.3 Hz, 1H, H-1′α), 2.05−2.00 (m, 1H, H-11β), 1.94 (s, 3H, H-27), 1.87−1.77 (m, 8H, H-11α, H-20′β, H-21′, H-28′α, H-29′α, H-34′), 1.74−1.68 (m, 1H, H-28′β), 1.66−1.58 (m, 1H, H-20α), 1.42−1.35 (m, 1H, H-35′α), 1.34−1.28 (m, 1H, H-20β), 1.20−1.15 (m, 1H, H-2′), 1.05−0.98 (m, 1H, H-35′β), 0.86 (t, J = 7.6 Hz, 3H, H-22′), 0.80 (d, J = 6.5 Hz, 3H, H-37′), 0.73 (t, J = 7.5 Hz, 3H, H-21), 0.72 (t, J = 7.5 Hz, 3H, H-36′). ^{13}C NMR (150 MHz, CD_3CN) δ (ppm) 176.0 (C-38′), 175.7 (C-31′), 173.2 (C-23′), 172.0 (C-24), 171.9 (C-50′), 171.7 (C-42′), 171.5 (C-26), 159.6 (C-16), 154.3 (C-18), 141.4 (C-4′), 137.3 (C-52′), 137.1 (C-44′), 136.6 (C-16′), 133.2 (C-18′), 131.6 (C-6), 131.3 (C-11′), 129.8 (C-46′, C-48′, C-54′ and C-56′), 129.5 (C-45′, C-49′, C-53′ and C-55′), 129.4 (C-47′ and C-55′), 125.8 (C-14), 125.7 (C-7), 125.0 (C-13), 124.6 (C-3′), 122.9 (C-14′), 122.3 (C-15′ and C-15), 120.7 (C-12′), 119.8 (C-13′), 117.0 (C-10′), 95.4 (C-17), 84.6 (C-2), 80.9 (C-3), 77.7 (C-4), 69.7 (C-30′), 68.2 (C-43′), 67.7 (C-51′), 66.4 (C-19), 64.2 (C-25′), 58.8 (C-5′), 58.4 (C-33′), 57.5 (C-22), 57.3 (C-19′), 57.1 (C-27′), 56.3 (C-7′), 54.8 (C-20′), 54.5 (C-12), 52.9 (C-25), 52.9 (C-24′), 51.5 (C-8), 51.1 (C-10), 49.9 (C-40′), 45.9 (C-11), 44.0 (C-5), 42.3 (C-8′), 39.2 (C-23), 38.7 (C-34′), 37.3 (C-41′), 36.8 (C-2′), 35.9 (C-1′), 32.2 (C-20), 31.6 (C-29′), 28.4 (C-21′), 27.3 (C-9′), 25.9 (C-35′), 25.6 (C-28′), 21.6 (C-27), 16.3 (C-37′), 13.1 (C-22′), 12.1 (C-36′), 9.2 (C-21). HRMS (ESI) calcd for $C_{77}H_{96}N_7O_{14}$ 1342.7010, found 1342.7078; $[\alpha]_D$ +12 ($CHCl_3$, c 1.0.)

Modeling. Molecular modeling studies were performed using crystal structures 1Z2B[3a] and the 3DU7[6] (PDB codes).

■ ASSOCIATED CONTENT

Ⓢ Supporting Information

Procedures for the molecular dynamics simulation of **22**, docking experiments, inhibition of tubulin assembly measurement, cell culture and proliferation assay, ^{1}H and ^{13}C NMR spectra for **12**, **20**−**22**, NOE spectrum for **22**, and full minimized structures of both epimers of **22**. This material is available free of charge via the Internet at http://pubs.acs.org.

■ AUTHOR INFORMATION

Corresponding Author

*Phone: + 0033 (0)1 69 82 31 21. Fax: + 0033 (0)1 69 07 72 47. E-mail: fanny.roussi@cnrs.fr.

Notes

The authors declare no competing financial interest.

■ ACKNOWLEDGMENTS

Jacques Fahy (Pierre Fabre Laboratories) is gratefully acknowledged for a generous gift of vinorelbine. O.G. gratefully acknowledges the ED425 "Innovation Thérapeutique, du Fondamental à l'Appliqué" for a grant and L'Oréal Foundation, UNESCO, and the French Academy of Science for her "Pour les Femmes et la Science" prize.

■ ABBREVIATIONS USED

VLB, vinblastine; VLN, vinorelbine; TBAF, tributylammonium fluoride; DMA, dimethylamine

■ REFERENCES

(1) Chen, S.-M.; Meng, L.-H.; Ding, J. New microtubule-inhibiting anticancer agents. *Expert Opin. Invest. Drugs* **2010**, *19*, 329−343.

(2) Stanton, R. A.; Gernert, K. M.; Nettles, J. H.; Aneja, R. Drugs that target dynamic microtubules: a new molecular perspective. *Med. Res. Rev.* **2011**, *31*, 443−481.

(3) (a) Gigant, B.; Wang, C.; Ravelli, R. B. G.; Roussi, F.; Steinmetz, M. O.; Curmi, P. A.; Sobel, A.; Knossow, M. Structural basis for the regulation of tubulin by vinblastine. *Nature* **2005**, *435*, 519−522. (b) Ranaivoson, F. M.; Gigant, B.; Berritt, S.; Joullié, M.; Knossow, M. Structural plasticity of tubulin assembly probed by vinca-domain ligands. *Acta Crystallogr., Sect. D: Biol. Crystallogr.* **2012**, *68*, 927−934.

(4) (a) Culvenor, C. C. J.; Beck, A. B.; Clarke, A.; Cockrum, P. A.; Edgar, J. A.; Frahn, J. L.; Jago, M. V.; Lanigan, G. W.; Payne, A. L.; Peterson, J. E.; Petterson, D. S.; Smith, L. W.; White, R. R. Isolation of toxic metabolites of *Phomopsis leptostromiformis* responsible for lupinose. *Aust. J. Biol. Sci.* **1977**, *30*, 269−277. (b) Mackay, M. F.; Van Donkelaar, A.; Culvenor, C. C. J. The X-ray structure of phomopsin A, a hexapeptide mycotoxin. *J. Chem. Soc., Chem. Commun.* **1986**, 1219−1221.

(5) Lacey, E.; Edgar, J. A.; Culvenor, C. C. J. Interaction of phomopsin A and related compounds with purified sheep brain tubulin. *Biochem. Pharmacol.* **1987**, *36*, 2133−2138.

(6) Cormier, A.; Marchand, M.; Ravelli, R. B. G.; Knossow, M.; Gigant, B. Structural insight into the inhibition of tubulin by vinca domain peptide ligands. *EMBO Rep.* **2008**, *9*, 1101−1106.

(7) (a) Ngo, Q. A.; Roussi, F.; Cormier, A.; Thoret, S.; Knossow, M.; Guénard, D.; Guéritte, F. Synthesis and biological evaluation of vinca alkaloids and phomopsin hybrids. *J. Med. Chem.* **2009**, *52*, 134−142. (b) Ngo, Q. A.; Roussi, F.; Thoret, S.; Guéritte, F. Elaboration of simplified vinca alkaloids and phomopsin hybrids. *Chem. Biol. Drug Des.* **2010**, *75*, 284−294.

(8) Rannoux, C.; Roussi, F.; Martin, M.-T.; Guéritte, F. Elaboration of vinblastine hybrids using a reactive in situ generated *N*-carboxyanhydride. *Org. Biomol. Chem.* **2011**, *9*, 4873−4881.

(9) Gherbovet, O.; Coderch, C.; García Alvarez, M. C.; Bignon, J.; Thoret, S.; Martin, M.-T.; Guéritte, F.; Gago, F.; Roussi, F. Synthesis and biological evaluation of a new series of highly functionalized 7′-*homo*-anhydrovinblastine derivatives. *J. Med. Chem.* **2013**, *56*, 6088−6100.

(10) Stohlmeyer, M. M.; Tanaka, H.; Wandless, T. J. A stereospecific elimination to form dehydroamino acids: synthesis of the phomopsin tripeptide side chain. *J. Am. Chem. Soc.* **1999**, *121*, 6100−6101.

(11) Gotoh, H.; Sears, J. E.; Eschenmoser, A.; Boger, D. New insights into the mechanism and an expanded scope of the Fe(III)-mediated vinblastine coupling reaction. *J. Am. Chem. Soc.* **2012**, *134*, 13240−13243.